A Blind Selected Mapping Technique for Low-PAPR Single-Carrier Signal Transmission

Amnart Boonkajay* and Fumiyuki Adachi†
*†Department of Communications Engineering, Graduate School of Engineering, Tohoku University
6-6-05 Aza-Aoba, Aramaki, Aoba-ku, Sendai, Miyagi, 980-8579 Japan
E-mail: *amnart@mobile.ecei.tohoku.ac.jp, †adachi@ecei.tohoku.ac.jp

***Abstract*—Single-carrier (SC) signals have a low peak-to-average power ratio (PAPR) property. However, the PAPR becomes higher as the modulation level increases. We have recently proposed a frequency-domain selected mapping (FD-SLM) which can effectively reduce PAPR of SC signal with high modulation level, but standard SLM technique requires the transmission of side-information to the receiver side. In this paper, a new FD-SLM with minimum mean-square error (MMSE) based blind signal detection is proposed, where there is no change on SLM algorithm at the transmitter and no necessity of side-information transmission. Simulation results show that the proposed blind FD-SLM technique reduces the PAPR of SC signals without significant degradation of bit-error rate (BER) performance.**

***Index Terms*—Single-carrier (SC) transmission, selected mapping (SLM), peak-to-average power ratio (PAPR)**

I. Introduction

Distributed antenna network (DAN) [1], which achieves high spectrum efficiency (SE) and energy efficiency (EE), is considered as a promising network architecture for the fifth-generation (5G) system. Single-carrier (SC) transmission with frequency-domain equalization (FDE) [2] is robust against frequency-selective fading channel [3] and has low peak-to-average power ratio (PAPR) property [4]. The PAPR, however, becomes higher as the modulation level increases [5-6]. Even though DAN can reduce the transmit power due to shorter range of transmission, PAPR reduction remains a significant issue in 5G in order to further reduce the power consumption of linear power amplifier at the mobile terminal. The use of square-root raised cosine (SRRC) filter with roll-off factor is known to reduce the PAPR of SC signals, but it is not a spectrum-efficient solution.

By utilizing the fact that SC signal can be generated in the frequency-domain, i.e., by inserting discrete Fourier transform (DFT) as a linear precoder to conventional orthogonal frequency division multiplexing (OFDM) transmitter [7], we recently proposed a frequency-domain selected mapping (FD-SLM) [8]. In FD-SLM, many transmit block candidates are generated by applying phase rotation on subcarriers (similar to SLM in OFDM) after DFT. FD-SLM can effectively reduce the PAPR of SC signal, however, the transmission of side-information is required, which is not desirable.

SLM without explicit side-information has been widely studied for OFDM signal transmission, e.g., scrambling [9], modified block code [10], and pilot tone insertion [11]; but these techniques still require transmission of small amount of redundant bits. Blind detection based on maximum likelihood (ML) [12] can achieve optimal solution without transmitting redundant bits, but requires extremely high complexity. A suboptimal detection for blind SLM for OFDM transmission is proposed in [13], where the received symbol is detected by calculating the mean-square error (MSE) in frequency domain between received block candidates generated from each de-mapping pattern and original signal constellations, then select the candidate with the lowest MSE. It is shown in [13] that the proposed blind detection achieves similar BER performance compared to SLM with perfect side-information knowledge, but it requires some restrictions such as real-valued phase rotation (± 1) sequence cannot be used, which also results in increasing of computational complexity at the transmitter. Meanwhile, the blind detection proposed in [13] can also be adopted to SC-FDE with few modifications. An important advantage of the blind detection in SC-FDE, which is also confirmed in this paper, is that the real-valued phase rotation sequence can be used.

Motivated by the above discussions, this paper proposes a blind FD-SLM technique for SC-FDE. The received block candidates are generated from all possible phase rotation de-mapping in frequency domain, then the MSE is computed in time domain after inverse DFT (IDFT), which is different from OFDM. Performance of the proposed transmission scheme is evaluated by computer simulation to show that the low-PAPR transmission is accomplished without significant BER performance degradation.

The rest of this paper is organized as follows. Transmitter model and its signal representation, including FD-SLM, are presented in Sect. II. Receiver with blind detection is presented in Sect. III. Section IV presents the simulation results, and Sect. V concludes the paper.

II. Transmitter with FD-SLM

An explanation of FD-SLM algorithm and its implementation in the transmitter is provided. Transmit and received signal blocks are represented as column vectors, and the signal processing in each stage is represented by matrix throughout this paper.

A. FD-SLM Algorithm

FD-SLM algorithm considered in this paper is similar to [8]. The phase rotation is applied to subcarriers prior to inverse fast Fourier transform (IFFT) operation.

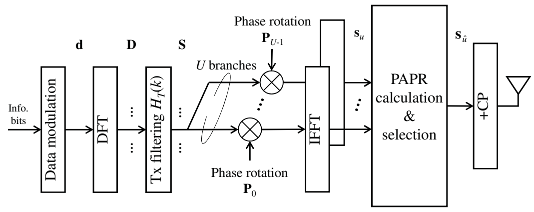

(a) SC-FDE transmitter with FD-SLM

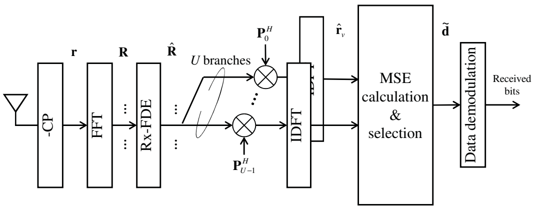

(b) SC-FDE receiver with blind detection

Fig. 1. Transceiver system model.

Assuming that an N_c-length time-domain transmit block is represented by a vector $\mathbf{s} = [s(0), s(1), \ldots, s(N_c-1)]^T$, PAPR is calculated over an oversampled transmission block, which is

$$\text{PAPR}(\mathbf{s}) = \frac{\max\{|s(n)|^2, n = 0, \frac{1}{V}, \frac{2}{V}, \ldots, N_c - 1\}}{E[|s(n)|^2]}. \qquad (1)$$

where V is oversampling factor (note that oversampling is necessary to accurately evaluate the PAPR).

A set of U different $N_c \times N_c$ diagonal matrices representing phase rotation $\mathbf{P}_u = diag[P_u(0), \ldots, P_u(N_c-1)], u = 0 \sim U-1$ is defined. Time-domain transmit block candidates are generated by multiplying the phase-rotation matrix to the frequency-domain components after transmit filtering and before IFFT, yielding $\mathbf{s}_u = \mathbf{F}_{N_c}^H \mathbf{P}_u \mathbf{H}_T \mathbf{F}_{N_c} \mathbf{d}$ where $\mathbf{H}_T$ and $\mathbf{F}_{N_c}$ represent transmit filtering and N_c-point DFT operations, respectively. The vector $\mathbf{d} = [d(0), \ldots, d(N_c-1)]^T$ represents the time-domain transmit symbols block. The instantaneous PAPR of $\mathbf{s}_u$ is calculated by referencing (1). In addition, oversampled version of $\mathbf{s}_u$ is obtained by padding $(V-1)N_c$ zeros to the frequency-domain signal vector $\mathbf{P}_u \mathbf{H}_T \mathbf{F}_{N_c} \mathbf{d}$ and then, applying VN_c-point IFFT. The selected transmit signal $\mathbf{s}_{\hat{u}} = [s_{\hat{u}}(0), \ldots, s_{\hat{u}}(N_c-1)]^T$ with the corresponding selected phase-rotation sequence index $\hat{u}$, whose provides the lowest PAPR among U candidates, is determined by the following criterion.

$$\hat{u} = \arg \min_{u=0,1,\ldots,U-1} \text{PAPR}(\mathbf{s}_u = \mathbf{F}_{N_c}^H \mathbf{P}_u \mathbf{H}_T \mathbf{F}_{N_c} \mathbf{d}). \qquad (2)$$

The matrix representations for transmit signal processing will be described in more details in Section II-B. Note that the transmitter with FD-SLM requires more computational complexity because of additional IFFT operations.

B. Transmit Signal Representation

Single-user N_c-length SC-FDE block transmission with N_g-length cyclic prefix (CP) insertion is considered in this paper. DFT and its inverse operation are employed for reaching subcarrier processing. Transmitter of SC-FDE using FD-SLM is illustrated by Fig. 1(a).

We begin with a block consisting of N_c data-modulated symbols $\mathbf{d} = [d(0), \ldots, d(N_c-1)]^T$. The block $\mathbf{d}$ is transformed into frequency domain by N_c-point DFT, yielding the frequency-domain signal vector $\mathbf{D} = [D(0), \ldots, D(N_c-1)]^T$ as

$$\mathbf{D} = \mathbf{F}_{N_c} \mathbf{d}, \qquad (3)$$

where the N_c-point DFT matrix $\mathbf{F}_{N_c}$ is given by

$$\mathbf{F}_{N_c} = \frac{1}{\sqrt{N_c}} \begin{bmatrix} 1 & 1 & \cdots & 1 \\ 1 & e^{\frac{-j2\pi(1)(1)}{N_c}} & \cdots & e^{\frac{-j2\pi(1)(N_c-1)}{N_c}} \\ \vdots & \vdots & \ddots & \vdots \\ 1 & e^{\frac{-j2\pi(N_c-1)(1)}{N_c}} & \cdots & e^{\frac{-j2\pi(N_c-1)(N_c-1)}{N_c}} \end{bmatrix}, \qquad (4)$$

and its Hermitian transpose $\mathbf{F}_{N_c}^H$ represents inverse operation.

Next, $\mathbf{D}$ is multiplied by an $N_c \times N_c$ transmit filtering matrix $\mathbf{H}_T = diag[H_T(0), \ldots, H_T(N_c-1)]$. We assume the transmit filtering in this paper to be SRRC filtering with roll-off factor α=0, i.e. ideal rectangular filtering, resulting in $H_T(k) = 1$ for all $k = 0 \sim N_c - 1$. The frequency-domain filtered signal vector $\mathbf{S} = [S(0), \ldots, S(N_c-1)]^T$ is represented by

$$\mathbf{S} = \mathbf{H}_T \mathbf{F}_{N_c} \mathbf{d}. \qquad (5)$$

The filtered signal $\mathbf{S}$ is then used as input signal in FD-SLM algorithm as described in Sect. II-A. The candidates are generated through U branches by multiplying $\mathbf{S}$ with $\mathbf{P}_u, u = 0 \sim U-1$, following by IFFT operation for obtaining the time-domain transmit block candidates $\mathbf{s}_u$. Selection is employed by referencing to (2) for obtaining the time-domain transmit block providing the lowest PAPR among U candidates as transmit signal, i.e. $\mathbf{s}_{\hat{u}}$, with the selected phase-rotation sequence $\mathbf{P}_{\hat{u}}$. In summary, $\mathbf{s}_{\hat{u}}$ can be expressed as

$$\mathbf{s}_{\hat{u}} = \mathbf{F}_{N_c}^H \mathbf{P}_{\hat{u}} \mathbf{H}_T \mathbf{D} = \mathbf{F}_{N_c}^H \mathbf{P}_{\hat{u}} \mathbf{H}_T \mathbf{F}_{N_c} \mathbf{d}. \qquad (6)$$

In case that $\mathbf{H}_T$ is ideal rectangular filter, (6) can be simplified as $\mathbf{s}_{\hat{u}} = \mathbf{F}_{N_c}^H \mathbf{P}_{\hat{u}} \mathbf{F}_{N_c} \mathbf{d}$. Finally, the last N_g samples of transmit block are copied as a CP and inserted into the guard interval (GI), then a CP-inserted signal block of $N_g + N_c$ samples is transmitted. We also would like to mentioned that there is no side-information sharing.

III. Receiver with Blind Detection

In this section, received signal representation and blind detection algorithm without side-information are described. The blind detection algorithm based on MSE calculation for OFDM transmission was proposed in [13], while the blind detection for SC-FDE transmission is proposed by this paper.

A. Received Signal Representation

Receiver block diagram with blind detection is illustrated by Fig. 1(b). The wireless propagation channel is assumed to be a symbol-spaced L-path frequency-selective block Rayleigh fading channel [3], where its impulse response is given by

$$h(\tau) = \sum_{l=0}^{L-1} h_l \delta(\tau - \tau_l), \tag{7}$$

where h_l and τ_l are complex-valued path gain and time delay of the l-th path, respectively. $\delta(\cdot)$ is the delta function. Time-domain received signal vector after CP removal $\mathbf{r} = [r(0), \ldots, r(N_c - 1)]^T$ is expressed by

$$\mathbf{r} = \sqrt{\frac{2E_s}{T_s}} \mathbf{h}\mathbf{s}_{\hat{u}} + \mathbf{n}, \tag{8}$$

where $\mathbf{s}_{\hat{u}} = \mathbf{F}_{N_c}^H \mathbf{P}_{\hat{u}} \mathbf{H}_T \mathbf{F}_{N_c} \mathbf{d}$ is obtained from (6). E_s is symbol energy, and $\mathbf{n}$ is noise vector in which each element is zero-mean additive white Gaussian noise (AWGN) having the variance $\frac{2N_0}{T_s}$ with T_s is symbol duration and N_0 being the one-sided noise power spectrum density. Channel response matrix $\mathbf{h}$ is a circular matrix representing time-domain channel response, which is

$$\mathbf{h} = \begin{bmatrix} h_0 & & & h_{L-1} & \cdots & h_1 \\ h_1 & \ddots & & & \ddots & \vdots \\ \vdots & & h_0 & \mathbf{0} & & h_{L-1} \\ h_{L-1} & & h_1 & \ddots & & \\ & \ddots & \vdots & & \ddots & \\ \mathbf{0} & & h_{L-1} & \cdots & \cdots & h_0 \end{bmatrix}. \tag{9}$$

The received signal in (8) is transformed into frequency domain by N_c-point fast Fourier transform (FFT), obtaining the frequency-domain received signal $\mathbf{R} = [R(0), \ldots, R(N_c - 1)]^T$ as

$$\begin{aligned} \mathbf{R} &= \sqrt{\tfrac{2E_s}{T_s}} \mathbf{F}_{N_c} \mathbf{h}\mathbf{s}_{\hat{u}} + \mathbf{F}_{N_c}\mathbf{n} \\ &= \sqrt{\tfrac{2E_s}{T_s}} \mathbf{F}_{N_c} \mathbf{h} \mathbf{F}_{N_c}^H \mathbf{P}_{\hat{u}} \mathbf{H}_T \mathbf{D} + \mathbf{F}_{N_c}\mathbf{n} \\ &= \sqrt{\tfrac{2E_s}{T_s}} \mathbf{H}_c \mathbf{H}_T \mathbf{P}_{\hat{u}} \mathbf{D} + \mathbf{N} \end{aligned}, \tag{10}$$

where the frequency-domain channel response $\mathbf{H}_c$ is defined by $\mathbf{H}_c \equiv diag[H_c(0), \ldots, H_c(N_c - 1)] = \mathbf{F}_{N_c} \mathbf{h} \mathbf{F}_{N_c}^H$.

FDE based on minimum MSE criterion (MMSE-FDE) [1] matrix $\mathbf{W}_R = diag[W_R(0), \ldots, W_R(N_c - 1)]$ is applied at the receiver in order to mitigate the effect from frequency selectivity. The equalized signal $\hat{\mathbf{R}} = \mathbf{W}_R \mathbf{R}$ is obtained, where the FDE weight at subcarrier k, $W_R(k)$, is determined by

$$W_R(k) = \frac{H_c^*(k) H_T^*(k)}{|H_c(k) H_T(k)|^2 + (E_s/N_0)^{-1}}. \tag{11}$$

It is observed from (11) that the FDE weight is derived in order to compensate the channel frequency selectivity only, while phase rotation de-mapping is not included, which is different from the FDE weight in [8]. This is because the selected phase-rotation sequence $\mathbf{P}_{\hat{u}}$ is still unknown. A signal detection without information of $\mathbf{P}_{\hat{u}}$, i.e. blind detection, will be introduced in the next subsection.

B. Blind Detection Algorithm

The blind detection algorithm can be briefly described as generating the received candidates from all possible phase rotation de-mapping in frequency domain, then select a candidate based on MSE calculation in time domain, where the one with the lowest MSE is selected as received signal. The algorithm is also illustrated together with the receiver block diagram in Fig. 1(b). By referencing (11), the frequency-domain equalized signal can be rewritten as

$$\hat{\mathbf{R}} = \mathbf{W}_R \mathbf{H}_c \mathbf{H}_T \mathbf{P}_{\hat{u}} \mathbf{D} + \mathbf{W}_R \mathbf{N}. \tag{12}$$

Next, U received signal vector candidates are generated in frequency domain, where the v-th frequency-domain received signal candidate $\hat{\mathbf{R}}_v = [\hat{R}_v(0), \ldots, \hat{R}_v(N_c - 1)]^T, v = 0 \sim U-1$ is generated by multiplying with the Hermitian transpose of corresponding v-th phase-rotation matrix $\mathbf{P}_v^H$, which is equivalent to de-mapping, that is

$$\hat{\mathbf{R}}_v = \mathbf{P}_v^H \hat{\mathbf{R}} = \mathbf{P}_v^H \mathbf{W}_R \mathbf{H}_c \mathbf{H}_T \mathbf{P}_{\hat{u}} \mathbf{D} + \mathbf{P}_v^H \mathbf{W}_R \mathbf{N}. \tag{13}$$

$\hat{\mathbf{R}}_v$ is then transformed back into time domain by N_c-point IDFT, yielding the time-domain received symbol vector candidate $\hat{\mathbf{r}}_v = [\hat{r}_v(0), \ldots, \hat{r}_v(N_c - 1)]^T$ as

$$\hat{\mathbf{r}}_v = \mathbf{F}_{N_c}^H \hat{\mathbf{R}}_v = \mathbf{F}_{N_c}^H \mathbf{P}_v^H \hat{\mathbf{R}}. \tag{14}$$

A suboptimal matric calculation and selection are conducted simultaneously in time domain for selecting which received vector candidate is likely to be de-mapped correctly. The time-domain received vector before de-modulation $\tilde{\mathbf{d}} = [\tilde{d}(0), \ldots, \tilde{d}(N_c - 1)]^T$ is decided by calculating the MSE between the received candidates and the nearest constellation points, then select the one providing the lowest MSE. MSE calculation and selection criterion can be expressed by the following equation.

$$\tilde{\mathbf{d}} = \min_{\substack{\hat{\mathbf{r}}_v, v \in \{0,1,\ldots,U-1\} \\ \tilde{d}(n) \in \Psi_{\text{mod}}}} \frac{1}{N_c} \sum_{n=0}^{N_c-1} |\hat{r}_v(n) - \tilde{d}(n)|^2, \tag{15}$$

where Ψ_{mod} is a set of constellations for each modulation level, for example, $\Psi_{\text{mod}} = \{\frac{3}{\sqrt{10}} + j\frac{3}{\sqrt{10}}, \frac{3}{\sqrt{10}} + j\frac{1}{\sqrt{10}}, \ldots, -\frac{3}{\sqrt{10}} - j\frac{3}{\sqrt{10}}\}$ in case of 16-QAM.

However, it is also described in [13] by assuming OFDM transmission that the above blind detection algorithm can work effectively if the following restrictions are accomplished:

- The set of phase-rotation sequences $\{\mathbf{P}_u, u = 0 \sim U-1\}$, is fixed and known *a priori*.
- For a given $\mathbf{c} = [c(0), \ldots, c(N_c - 1)]^T, c(n) \in \Psi_{\text{mod}}$, and assuming OFDM transmission, the necessary condition is $c(n) P_u(n) \notin \Psi_{\text{mod}}$ for all n and u. This restriction implies that real-valued phase rotation (i.e. $P_u(n) = \pm 1$) cannot be used.

The first criterion is cleared by employing a shared codebook containing all phase-rotation matrices, which is also typically employed in transmission with side-information.

On the other hand, candidate generation from all possible de-mapping patterns and MSE calculation are employed in

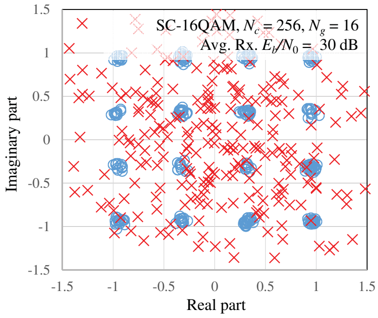

Fig. 2. One-shot observation of received candidates.

different domain in SC-FDE, i.e., candidate generation is applied to subcarrier and MSE calculation is done on time-domain received signal after IDFT. An inaccurate de-mapping in frequency domain is equivalent to residual ISI in time domain, yielding the MSE values obtained from different de-mapping patterns are sufficiently different even though real-valued phase rotation sequence is used. This summarizes that the second restriction can be neglected in case of SC-FDE.

In addition, Fig. 2 shows one-shot observation of $\hat{\mathbf{r}}_v$ assuming SC-FDE with 16-QAM modulation at average received bit energy-to-noise power spectrum density ratio E_b/N_0=30 dB. Note that $E_b/N_0 = (1/N_{\text{mod}})(E_s/N_0)(1 + N_g/N_c)$, where N_{mod} represents modulation level (4 for 16-QAM, and 6 for 64-QAM). It is seen that $\hat{r}_v(n)$ is very close to original 16-QAM constellations when $v = \hat{u}$, which results in very low MSE. On the other hand, $\hat{r}_v(n)$ is scattered over I-Q diagram when $v \neq \hat{u}$, which results in high MSE. This indicates that the above blind detection has a potential to achieves high accuracy when the received E_b/N_0 is sufficiently high.

IV. Performance Evaluation

Numerical and simulation parameters are summarized in Table I. We assume SC-FDE block transmission with the number of available subcarriers N_c=64. Oversampling factor is set to be V=8. System performances of conventional SC-FDE, SC-FDE using FD-SLM (with side-information sharing) and SC-FDE using blind FD-SLM are evaluated in terms of PAPR of transmit signal, average BER (uncoded), and throughput.

A. PAPR Performance

PAPR performance is evaluated by measuring the PAPR value at complementary cumulative distribution function (CCDF) equals 0.001, called $\text{PAPR}_{0.1\%}$, where its definition is expressed by $prob(\text{PAPR}(\mathbf{s}) \geq \text{PAPR}_{0.1\%}) = 0.001$.

Fig. 3 shows the $\text{PAPR}_{0.1\%}$ performances of SC-FDE using blind FD-SLM as a function of number of candidates (U) and with various data modulation levels (i.e. QPSK, 16-QAM, and 64-QAM). The $\text{PAPR}_{0.1\%}$ of conventional SC-FDE (i.e. SC-FDE with rectangular filtering) is shown at the place with U=0. It is observed from Fig. 3 that $\text{PAPR}_{0.1\%}$ decreases when U increases, which is same as performance of FD-SLM in [8] since there is no changes on SLM algorithm at the transmitter.

TABLE I
Simulation parameters.

Transmitter	Modulation	QPSK, 16QAM, 64QAM
	FFT/IFFT block size	N_c = 64
	Cyclic prefix length	N_g = 16
	Phase rotation sequence type	4095-bit long PN
	No. of candidates	U = 1(no SLM)∼512
	$\text{PAPR}_{0.1\%}$ threshold	6 dB
Channel	Fading type	Frequency-selective block Rayleigh
	Power delay profile	symbol-spaced 16-path uniform
Receiver	Channel estimation	Ideal
	Side-information sharing	FD-SLM → Ideal detection Blind FD-SLM → No SI
	FDE	MMSE-FDE

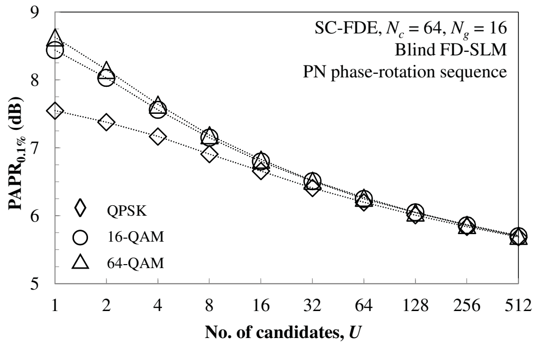

Fig. 3. PAPR versus number of candidates.

B. BER Performance

BER performance as a function of average received E_b/N_0 of SC-FDE using blind FD-SLM are shown in Fig. 4, and compared to SC-FDE using FD-SLM with ideal side-information detection at U=64. It can be seen from every modulation schemes that the BER performances slightly degrade when U increases at low received E_b/N_0 region. The reason behind this degradation can be described by referencing Sect. III-B and Fig. 2, as the effect from noise power makes the received signal become apart from original constellations even though the de-mapping is accurately organized. This makes the MSE value of the time-domain received candidates with accurate de-mapping become insufficiently different from the one with inaccurate de-mapping.

However, it can be seen that there is no significant degradation on BER when $E_b/N_0 \geq 10$ dB for 16-QAM, and $E_b/N_0 \geq 8$ dB for 64-QAM. These results confirm that the proposed blind detection for SC-FDE can be used effectively when the received E_b/N_0 is sufficiently high.

C. Throughput Performance

Throughput performance of SC-FDE using blind FD-SLM algorithm are evaluated as a function of peak transmit E_s/N_0, where the throughput performance in bps/Hz is defined as follows [5].

$$\eta = N_{\text{mod}} \times (1 - \text{PER}) \times \frac{1}{1+\alpha} \times \frac{1}{1 + \frac{N_g + N_{SI}}{N_c}}. \qquad (16)$$

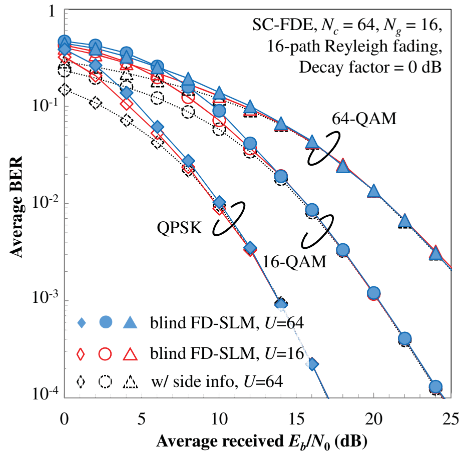

Fig. 4. BER performances.

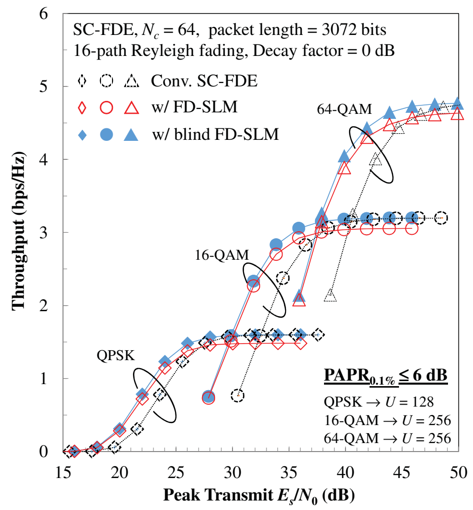

Fig. 5. Throughput performances.

where PER is packet-error rate and N_{SI} is the number of required side-information symbols, which is assumed to be $N_{SI} = \lceil (\log_2 U)/N_{\text{mod}} \rceil$. The packet length is assumed to be 3072 bits in this paper. The peak transmit E_s/N_0 is considered since it refers to the required peak transmit power of a power amplifier (PA), while the peak transmit E_s/N_0 is defined as a summation of average received E_s/N_0 and $\text{PAPR}_{0.1\%}$ [5].

Fig. 5 shows the average throughput performances of SC-FDE using conventional FD-SLM with ideal side-information detection and SC-FDE using blind FD-SLM. The number of candidates is set as the minimum U for achieving $\text{PAPR}_{0.1\%} \leq 6$ dB, i.e., U equals 128, 256 and 256 for QPSK, 16-QAM and 64-QAM, respectively. SC-FDE using FD-SLM with side-information provides better throughput performance at low peak E_s/N_0 region compared to conventional SC-FDE as a contribution from low-PAPR signal, but there is a small degradation of peak throughput. On the other hand, SC-FDE using blind FD-SLM can provide similar throughput performance at low peak E_s/N_0 region compared to SC-FDE using conventional FD-SLM, but there is no degradation on peak throughput because no side-information sharing is required. We also would like to mention that the use of SRRC filter with roll-off factor α is able to reduce the PAPR, but also reduces the peak throughput by a factor of $1/(1+\alpha)$.

V. Conclusion

FD-SLM with blind detection algorithm based on MMSE for SC-FDE was proposed in this paper. The proposed blind detection algorithm generates received candidates via phase-rotation de-mapping in frequency domain and then calculates the MSE in time domain, which is different from the conventional blind detection in OFDM transmission. PAPR reduction performance can be achieved same as in [8]. Computer simulation results confirmed that SC-FDE transmission using the proposed blind FD-SLM achieved low-PAPR transmission without signification degradation on BER and throughput.

Acknowledgment

This research was funded by the national project of "Research and Development on 5G mobile communications system", supported by the Ministry of Internal Affairs and Communications (MIC), Japan.

References

[1] F. Adachi, K. Takeda, T. Yamamoto, R. Matsukawa and S. Kumagai, "Recent Advances in Single-Carrier Distributed Antenna Network," *Wiley Wireless Commun. and Moblie Comput.*, Vol. 11, pp. 1551-1563. Dec. 2011.

[2] D. Falconer, S. L. Ariyavisitakul, A. Benyamin-Seeyar and B. Edison, "Frequency domain equalization for single-carrier broadband wireless systems," *IEEE Commun. Mag.*, Vol. 40, No. 4, pp. 58-66. Apr. 2002.

[3] A. Goldsmith, *Wireless Communications*, Cambridge University Press, 2005.

[4] H. Sari, G. Karam and J. Jeanclaude, "Transmission Techniques for Digital Terrestrial TV Broadcasting," *IEEE Commun. Mag.*, Vol. 33, No. 2, pp. 100-109, Feb. 1995.

[5] S. Okuyama, K. Takeda and F. Adachi, "MMSE Frequency-domain Equalization Using Spectrum Combining for Nyquist Filtered Broadband Single-Carrier Transmission," *in Proc. IEEE Veh. Technol. Conference (VTC 2010-Spring)*, Taipei, Taiwan, May 2010.

[6] A. Boonkajay, T. Obara, T. Yamamoto and F. Adachi, "Performance Evaluation of Low-PAPR Transmit Filter for Single-Carrier Transmission," *in Proc. Asia-Pacific Conference on Commun. (APCC 2012)*, Jeju Island, Korea, Oct. 2012.

[7] D. Falconer, "Linear Precoding of OFDMA Signals to Minimize Their Instantaneous Power Variance," *IEEE Trans. Commun.*, Vol. 59, No. 4, pp. 1154-1162, Apr. 2011.

[8] A. Boonkajay, T. Obara, T. Yamamoto and F. Adachi, "Selective Mapping for Broadband Single-Carrier Transmission Using Joint Tx/Rx MMSE-FDE," *in Proc. IEEE Int. Symp. on Personal Indoor and Mobile Radio Commun. (PIMRC 2013)*, London, U.K., Sept. 2013.

[9] M. Breiling, S. Muller-Weinfurtner and J. Huber, "SLM Peak-Power Reduction without Explicit Side Information," *IEEE Commun. Lett.*, Vol. 5, No. 6, pp. 239-241, Jun. 2001.

[10] N. Carson and T. A. Gulliver, "PAPR Reduction of OFDM using Selected Mapping, Modified RA Codes and Clipping," *in Proc. IEEE Veh. Technol. Conference (VTC 2002-Fall)*, Vancouver, Canada, Sept. 2002.

[11] S. Y. Le Goff, S. S. Al-Samahi, B. K. Khoo, C. C. Tsimenidis and B. S. Sharif, "Selected Mapping without Side Information for PAPR Reduction in OFDM," *IEEE Trans. Wireless Commun.*, Vol. 8, No. 7, pp. 3320-3325, Jul. 2009.

[12] J. G. Proakis and M. Salehi, *Digital Communications*, 5^{th}ed., McGraw-Hill, 2008.

[13] A. D. S. Jayalath and C. Tellambura, "SLM and PTS peak-power reduction of OFDM signals without side information," *IEEE Trans. Wireless Commun.*, Vol. 4, No. 5, pp. 2006-2013, Sept. 2005.